AD A279395

Low Frequency Sound Radiation
From Finite Stiffened Plates

- LECTE
MAY 19 1994
B D
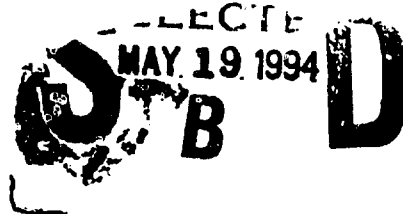
Report to:

Submitted by

Richard F. Keltie, Ph.D.

Center for Sound and Vibration
Department of Mechanical and Aerospace Engineering
North Carolina State University
Raleigh, North Carolina 27695-7003

July 28, 1993

94-14903

Table of Contents

I. Introduction

The purpose of the research effort reported herein was to assess the feasibility of developing efficient low frequency acoustic radiators using flexural vibration of submerged stiffened plates. The work conducted at North Carolina State University was performed in collaboration with Dr. Benjamin Cray of the Naval Undersea Warfare Center (NUWC), New London Detachment. Candidate radiator geometries were identified at NUWC using an infinite plate model [1]. A finite plate implementation of these models was then examined by the author using an analysis capability previously developed [2]. The purpose of this examination was to study the extent to which infinite plate results could be achieved by a finite radiator, and to obtain an estimate of the effects of plate size and number of attached ribs on the radiation characteristics.

Specific items of interest included calculation and comparison of the wavenumber-frequency spectra (k-ω) of the plate responses, examination of the change in radiated sound pressure level upon addition of attached ribs, and calculation of the far field directivity patterns in response to a line drive applied to the plate. In the sections below, the finite plate model is briefly reviewed, comparisons are shown between the infinite and finite plate predictions, and the results of a parameter study of finite plate behavior are presented for a candidate projector geometry.

II. Background - Finite Plate Model

The finite plate model consisted of a line-forced plate whose ends were taken to be restrained by simple supports. Because of the line-force assumption, the rib effects were modeled as simple inertial reactions acting normal to the plate's surface. The equation of motion for the plate response is given by:

$$D\frac{\partial^4 w(x)}{\partial x^4} - \rho h \omega^2 w(x) = F_0 \delta(x - x_0) - p_a(x,0) - \sum_{r=1}^{R} p_r(x) \qquad (1)$$

where D is the flexural stiffness, $w(x)$ is the plate transverse displacement, ρh is the plate mass per unit area, ω is the circular frequency of the applied force, F_0 is the force/length of the applied force, p_a is the acoustic pressure acting on one surface of the plate, p_r is the pressure arising from each rib's reaction, and R is the total number of ribs. The rib reactions are related to the plate's displacement through the equation:

$$p_r(x) = -m_r'\omega^2 w(x)\delta(x - x_r) \tag{2}$$

where m_r' is the mass/length of each rib and x_r is the location of each rib. In-plane and rotational effects of the ribs are neglected in this model, although non-uniformities in rib size and location are permitted.

The plate displacement response is expanded using orthonormal basis functions generated from the in-vacuo unstiffened plate modes. The plate displacement may be represented by the truncated expansion:

$$w(x) = \sum_{n=1}^{N} W_n \varphi_n(x) \tag{3}$$

The analysis effort then reduces to solving for the expansion coefficients, W_n. This involves solving an NxN system of algebraic equations [2,3]. The number of modes used in the expansion depends on the frequency, but it was always ensured that approximately 20-30 modes beyond the resonant fluid-loaded mode were included.

Once the surface displacement field is known, the radiated acoustic field may be obtained through use of the Rayleigh radiation integral:

$$p_a(x,z) = \rho_0\omega^2 \int_0^L g(x,z|x_0)w(x_0)dx_0 \tag{4}$$

where g is the appropriate Green's function [4]. The length of the plate is given by L, and semi-infinite rigid baffles are assumed to exist beyond either end of the plate's surface. This integral was evaluated numerically to examine the far field radiated sound

levels, and their directivity patterns. The calculated far field sound levels were adjusted to correspond to those referenced to a distance of $1m$ from the plate's surface.

It was also of interest to examine the wavenumber spectrum of the surface displacement response, $\overline{w}(k)$, defined by:

$$\overline{w}(k) = \int_0^L w(x)e^{-jkx}dx \tag{5}$$

Given the form of the plate displacement, Equation (3), it is clear that the wavenumber transforms of the *in-vacuo* mode shapes are required. These are given by:

$$\overline{\Phi}_n(k) = \left[1 - (-1)^n e^{-jkL}\right] \frac{\dfrac{n\pi}{L}}{\left(\dfrac{n\pi}{L}\right)^2 - k^2} \tag{6}$$

Using this result, the wavenumber spectra are obtainable directly from knowledge of the expansion coefficients, W_n. The wavenumber spectra of the finite plate mode shapes given by Equation (6) are seen to have their maximum value at the modal wavenumber, namely $n\pi/L$. The scattering of energy into other wavenumber components is due to truncation effects inherent in the finite domain of the structural response. In addition, it is clear that the upper limit to which meaningful wavenumber information may be obtained is directly proportional to the mode number, n.

III. Comparison Between Infinite and Finite Cases

The infinite plate model allows for rapid calculation of radiated sound pressure level as a function of frequency, and also for subsequent examination of the k-ω spectrum. After examining several plate geometries, a candidate for detailed comparison was chosen. This geometry consisted of a 1/8" (0.003175m) thick steel plate, with equally-spaced attached stiffeners each of which had a cross-sectional area of 0.443in^2

($2.857 \times 10^{-4} m^2$). The spacing between ribs was 8" ($0.2032m$). The line force was taken to have an amplitude of 68.5 *lb/ft* (1000 *N/m*) and was applied directly over a rib.

The radiated sound pressure level, in water, was calculated at a stand-off distance of 1*m* directly above the line force. The results, presented in Figure 1, show pronounced peaks in the radiated sound pressure level at discrete frequencies, the first of which occurs at 420 *Hz*. It may be shown that these frequencies coincide with those at which an integral number of stiffened plate bending waves fit between adjacent rib stiffeners. Thus, the presence of the ribs generates a mechanism whereby low frequency acoustic radiation is significantly enhanced. Comparison of these results with those obtained from an unribbed infinite plate, show that the peaks in the radiated pressure from the ribbed plate exceed those from the unribbed plate by approximately 20 *dB*.
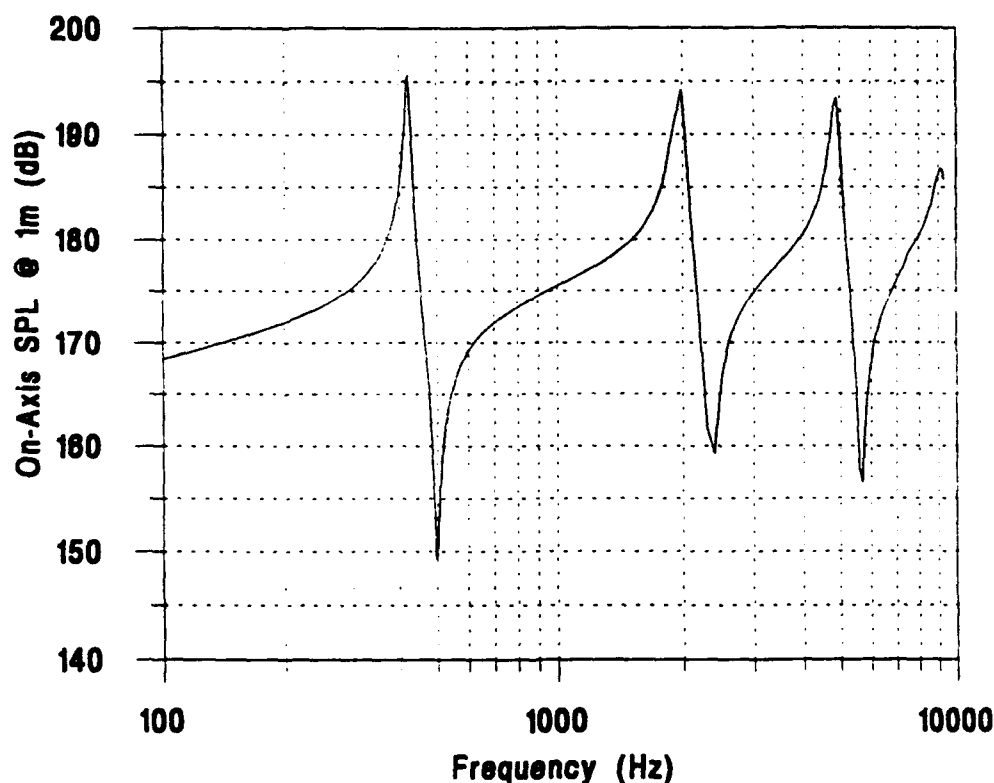

Figure 1. On-Axis Sound Pressure Level vs. Frequency for the Infinite Ribbed Plate.

The underlying reason for this enhanced radiation may be seen by examining the wavenumber spectrum of the plate response. The normalized wavenumber spectrum of the plate displacement, $W_r(k)$, at a frequency of $420Hz$ is shown in Figure 2. The dominant peaks at wavenumber values of $\pm 30m^{-1}$ are associated with the two traveling bending waves propagating away from the line force. These values of wavenumber are also associated with the rib-to-rib spacing on the plate. The vertical dashed lines indicate the acoustic wavenumber, $\pm k_0$. The sound radiation at $420Hz$ is produced solely due to the supersonic wavenumber components lying between the vertical dashed lines. It may be observed that there exists a concentration of energy at and near zero wavenumber.
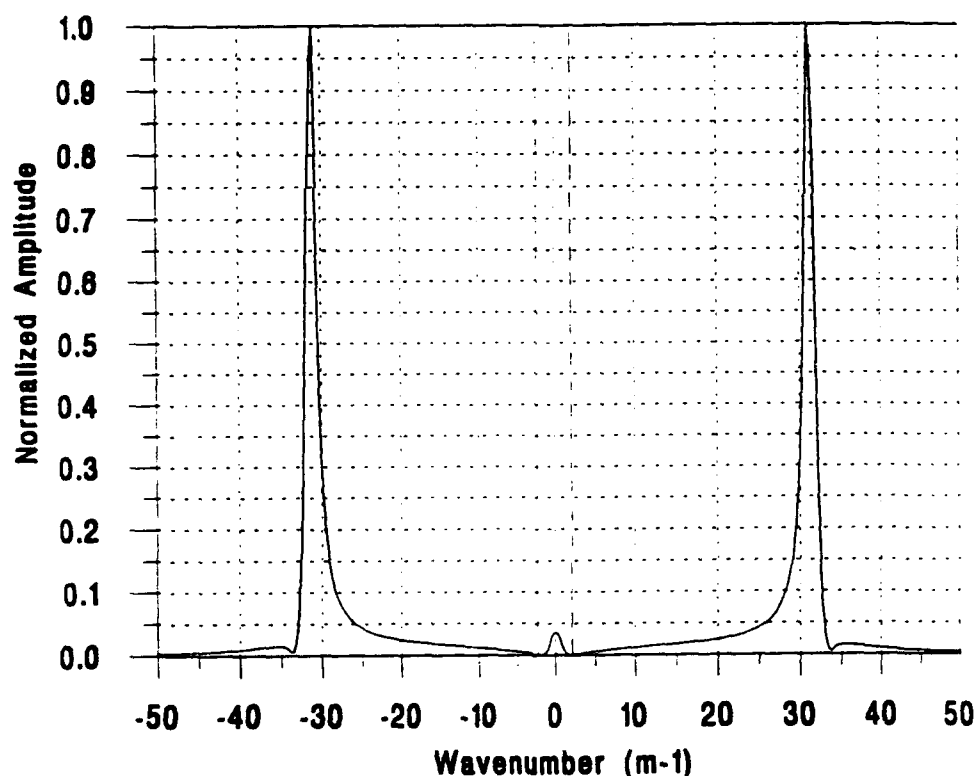

Figure 2. Normalized k-Spectrum for the Infinite Ribbed Plate at $420Hz$.

In order to show that this observation results from the presence of the attached ribs, Figure 3 presents the same wavenumber spectrum, although normalized in a different manner. In this data, the ribbed wavenumber spectrum, $W_r(k)$, has been divided

by the unribbed wavenumber spectrum, $W_{ur}(k)$. These results more clearly show the effects of the attached rib stiffeners, in that some of the supersonic wavenumber components have been increased in amplitude by an order of magnitude over the unribbed plate. These enhanced supersonic components are responsible for the increase in the radiated sound pressure levels.
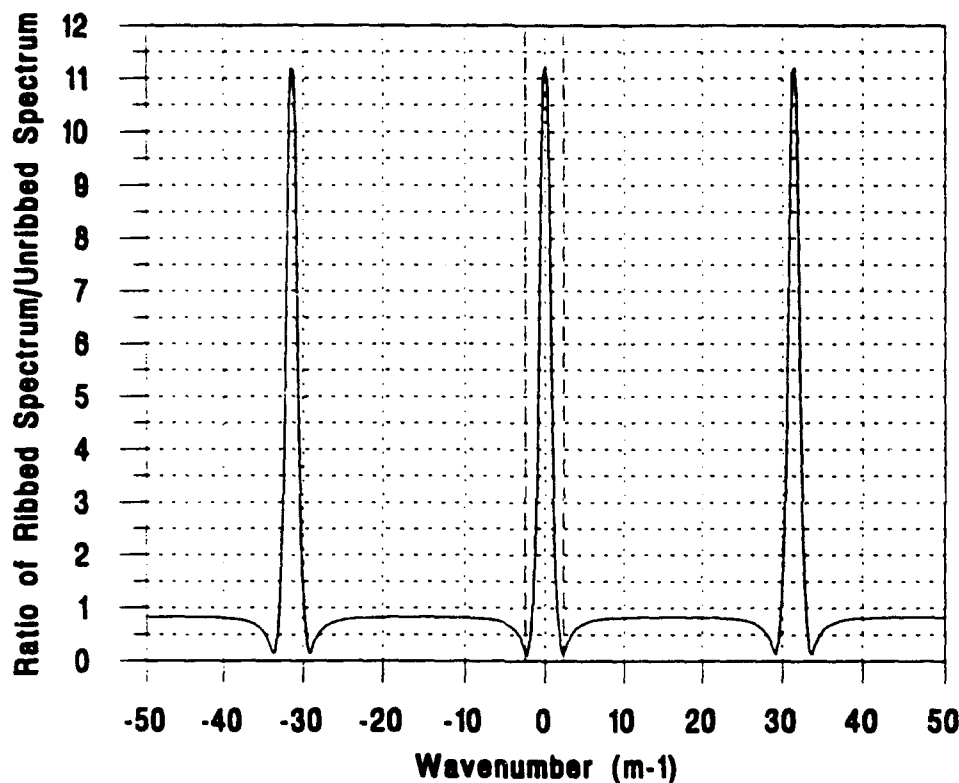

Figure 3. Ratio of k-Spectra (Ribbed/Unribbed) for the Infinite Plate at $420Hz$.

In order to determine if comparable effects could be obtained from a finite plate, it was decided to examine a 'long' plate designed to simulate the infinite case results. The model chosen involved a 48-ft (14.6304m) long plate with 71 attached ribs. The size and spacing of these ribs was the same as in the infinite case. The radiated on-axis sound pressure level, directly above the force location, is shown in Figure 4 over the frequency range 100-700Hz. These results may be compared with the infinite plate results in Figure 1. It should be noted that the restricted frequency range in the finite plate is a result of

the prohibitively large number of structural modes needed to calculate the response at high frequency for such a large plate.
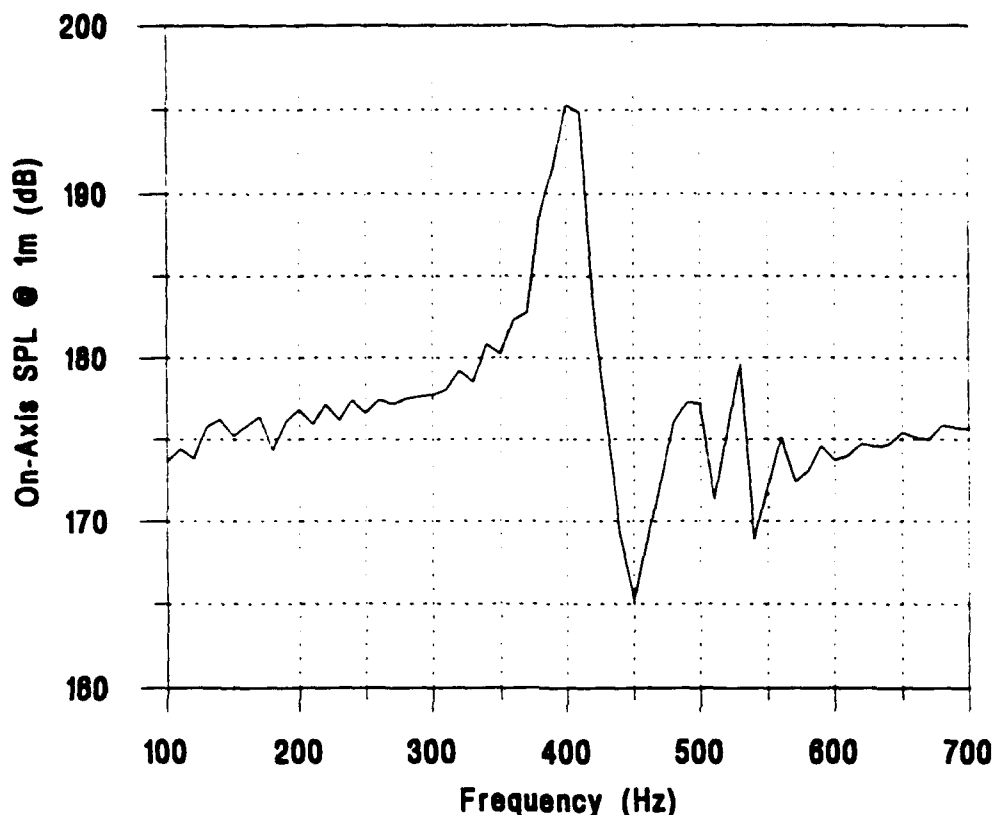

Figure 4. Radiated SPL vs. Frequency for 48-*ft* (14.6024*m*) Ribbed Plate

Nonetheless, the finite plate results demonstrate good agreement with the infinite plate results. Overall, both are typified by an increase in radiated sound pressure level, reaching a peak near 400*Hz*, followed by a pronounced minimum in the sound pressure. The peak in the finite plate results is a bit broader in frequency range and occurs at a slightly lower frequency. The broadening is undoubtedly due to the 'smearing' effects associated with a radiator of finite extent. The downward shift in frequency, by approximately 10*Hz*, remains unexplained since both models used identical values for the plate and water properties. A possible explanation may be found in boundary condition effects for the finite plate, but this was not pursued in detail. The general agreement,

however, between the shapes and amplitudes of the SPL vs. frequency results was the notable observation.

The frequency resolution used in obtaining the results shown in Figure 4 was 10*Hz*. In an attempt to more clearly define the specific frequency at which the peak in the sound pressure level occurs, a finer resolution scan utilizing a 1*Hz* increment was performed over a narrow frequency band. These results are shown in Figure 5. From this data it difficult to pick a specific frequency that corresponds to the observed behavior in the infinite plate results. In order to identify a specific frequency for detailed study, it was necessary to obtain some further indicator of frequency-dependent behavior. Guided by the infinite plate results, it was found to be helpful to examine the k-ω spectrum.
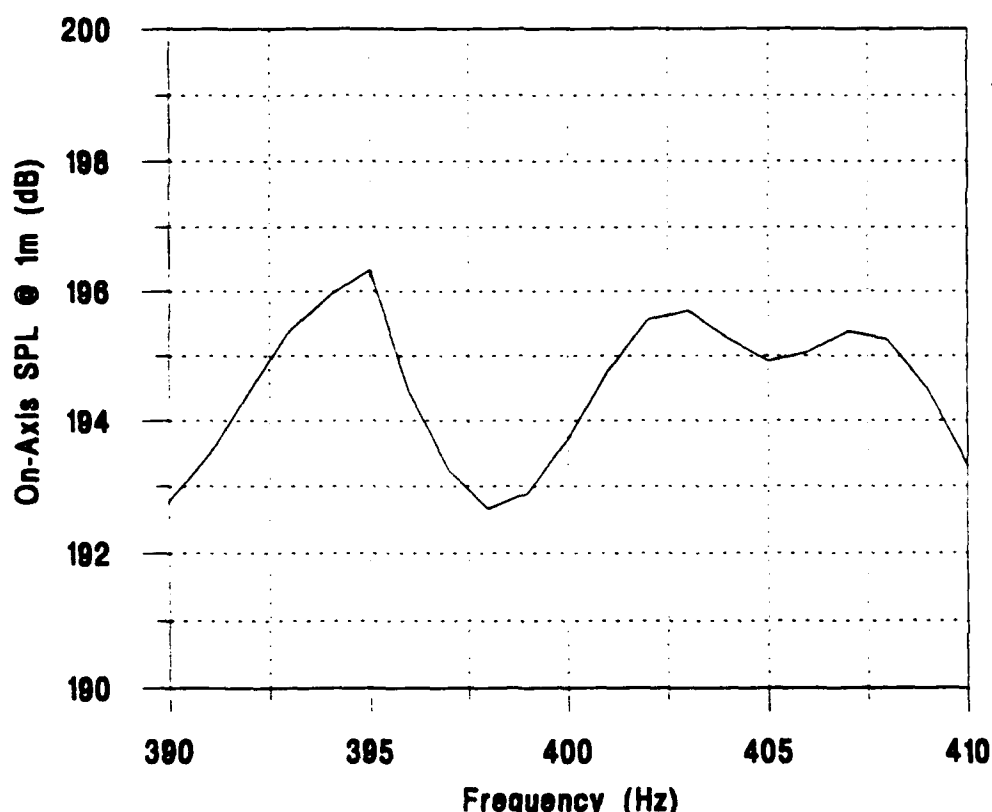

Figure 5. SPL vs. Frequency for 48-*ft* (14.6024*m*) Ribbed Plate (1*Hz* Resolution)

Figure 6 shows the k-ω spectrum for the finite plate displacement field over the frequency range covered in Figure 5. The displayed wavenumber range has been

restricted to the supersonic portion only. This data shows a clear peak in the low-wavenumber spectral amplitude at a frequency of 407Hz. Thus, this frequency is taken to be the finite plate counterpart of the 420Hz frequency observed in the infinite plate results earlier. Not only does the radiated sound pressure level have a near-maximum value at this frequency, but there is also a maximum value in the wavenumber spectrum at $k=0$. In the following section, detailed examinations of a variety of finite plates are made at this frequency value of 407Hz. These examinations are made to study the effects of plate size and rib numbers on the radiated sound pressure, the directivity of the radiation pattern, and the generation of significant energy in the supersonic wavenumber region.
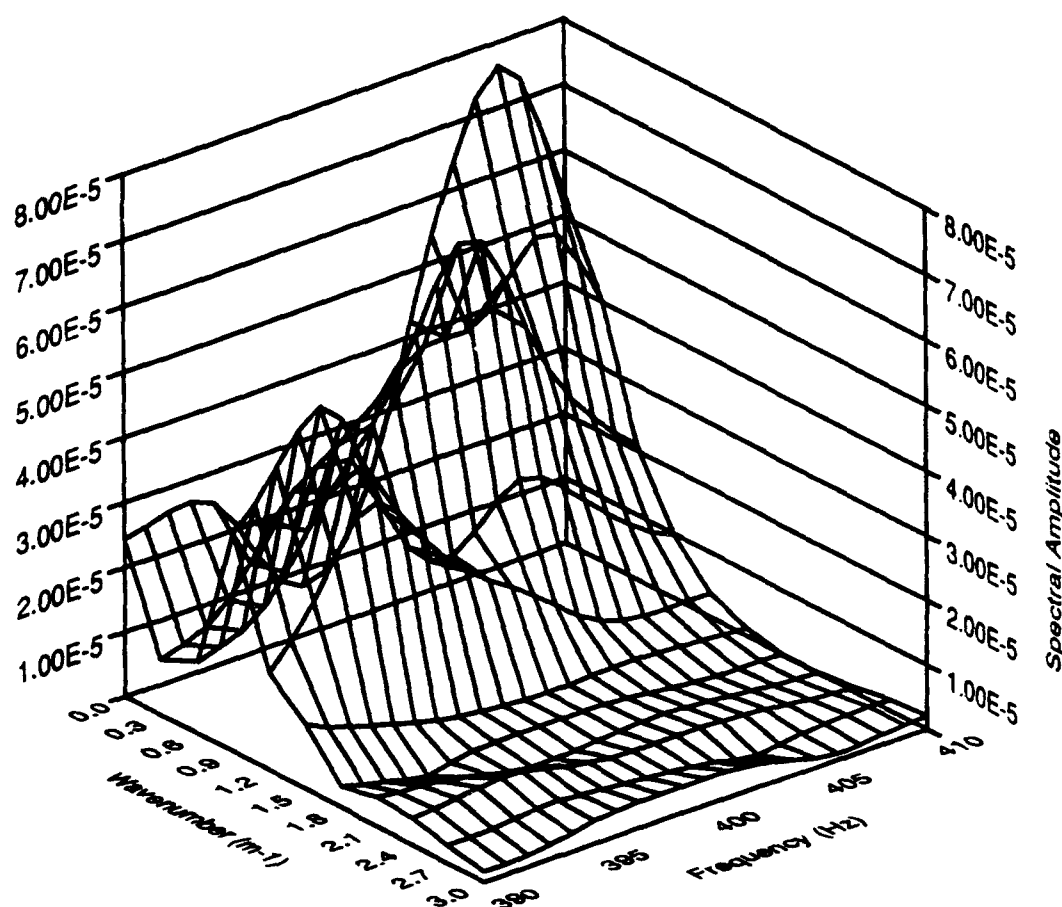
Figure 6. Portion of the k-ω Spectrum for 48-ft (14.6024m) Ribbed Plate

IV. Parameter Study of Candidate Plates

A total of six different finite plate models were examined. Each model consisted of an 1/8" (0.003175m) thick steel plate to which were attached different numbers of equally-spaced uniformly sized ribs. As in the infinite case, each rib had a cross-sectional area of 0.443in^2 (2.857x10$^{-4}m^2$), with a spacing between ribs of 8" (0.2032m). The number of ribs was chosen so that a rib was always located at the mid-length position. In this way, symmetry was preserved to assist in comparisons with the infinite plate results. A line force with the same amplitude of 1000 N/m was applied directly over this central rib. The pertinent data for these different cases is shown in Table 1. As discussed above, the response of each of these plates was examined at a frequency of 407Hz.

Table 1. Finite Plate Geometries

Plate Length	Non-Dimensional Plate Length, kL (407Hz)	Number of Ribs
8-ft (2.4384m)	4.157	11
16-ft (4.8768m)	8.314	23
24-ft (7.3152m)	12.470	35
32-ft (9.7536m)	16.627	47
40-ft (12.1920m)	20.784	59
48-ft (14.6304m)	24.941	71

IV-1. Radiated Sound Pressure Levels

The on-axis sound pressure levels for the six candidate plates were calculated at 407Hz. These calculations were made for both ribbed and unribbed plates. The results are shown in Figure 7 as a function of normalized plate length, kL. The effects of the attached ribs on the radiated sound level are dependent on the length of the plate, or more

appropriately, on the number of attached ribs. The shortest plate, the one with only 11 ribs, behaves very nearly the same as a similar unribbed plate. As the plate length is increased, the ribbed plate is seen to radiate considerably more sound. When the plate length has increased to 24-*ft* (7.3152*m*, *kL*=12.470), the sound level has increased essentially to that observed in the infinite ribbed plate results. Further increases in the plate length and number of ribs have negligible effect on the radiated sound.
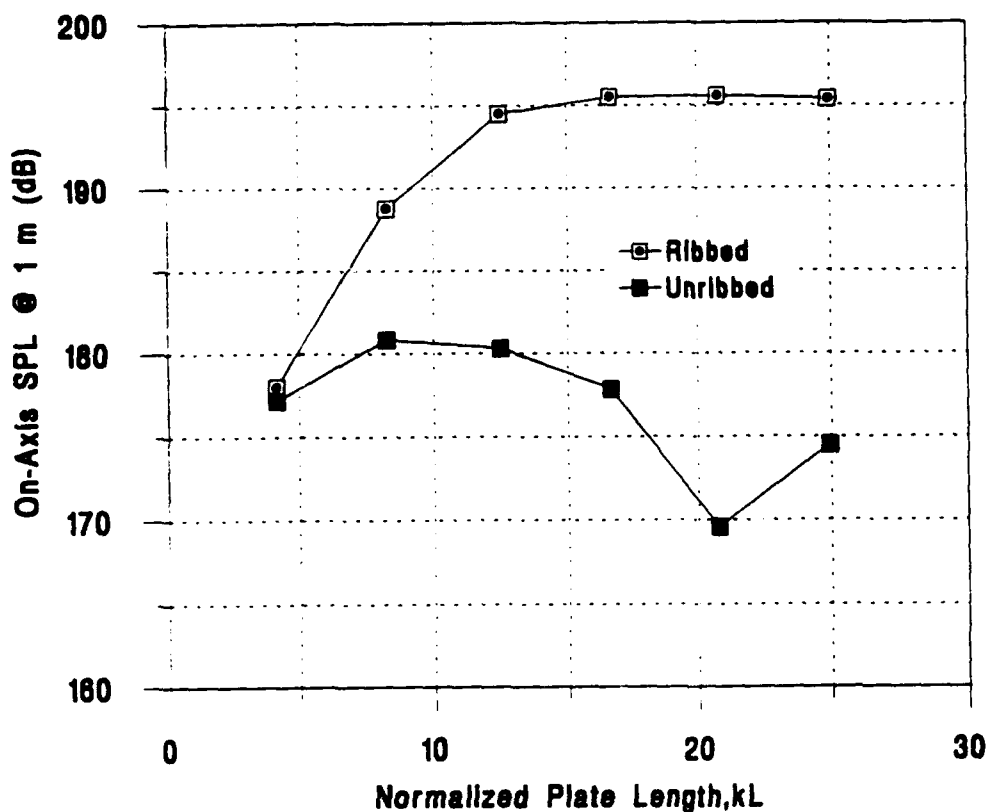

Figure 7. On-Axis Sound Pressure Level at 407*Hz* for Ribbed and Unribbed Plates.

In addition, it is seen that the ribbed plate radiates at least 15*dB* and as much as 25*dB* more than a similar unribbed plate at a frequency of 407*Hz*. While the unribbed plate shows variations in radiated sound level in Figure 7, most likely due to the effects of resonance on plate response, the sound levels radiated by the ribbed plates rapidly approach an asymptotic value. This value of radiated sound is very close to that predicted by the infinite plate model as seen in Figure 1. This observation would

indicate that the rib effects quickly dominate the resonance effects of the underlying plate at this frequency.

IV-2. k-ω Spectrum Effects

The normalized wavenumber spectra for the six finite plates are shown in Figures 8(a)-8(f) for an excitation frequency of 407Hz. In each case, the spectrum has been normalized to its maximum value which occurs near a wavenumber value of 30m^{-1}. Examination of these results show several trends. First, the oscillations in the spectral shapes are associated with the truncation effects resulting from the finite length of the plate. These oscillations quickly disappear as the length of the plate increases, and are essentially gone in Figure 8(c). Additional effects noted are the sharpening of the main peak, and the generation of supersonic wavenumber components near the origin, k=0. Similar to the decay of the truncation oscillations, these changes have nearly completely occurred by the time the plate length has increased to 24-ft (7.3152m, kL=12.470). Furthermore, comparison with Figure 2 shows that the wavenumber spectrum of the finite plate has also nearly matched that of the infinite plate.

In order to more easily assess the effect of plate length and rib number on the important supersonic portion of the wavenumber spectrum, an additional means of data analysis was employed. This involved the determination of the area, and hence the power, contained in the supersonic portion of the spectrum in each of the results shown in Figure 8. These values were then compared to similar values calculated for the unribbed plates, and the ratios are shown in Figure 9. These results show the effectiveness of the attached ribs in converting non-radiating response components in the unribbed plate to supersonic radiating components. The effect of plate length is seen to rise rapidly between the 24-ft (7.3152m, kL=12.470) and the 32-ft (9.7536m, kL=16.627) plates. This would indicate a 'critical plate length' occurring in this range.
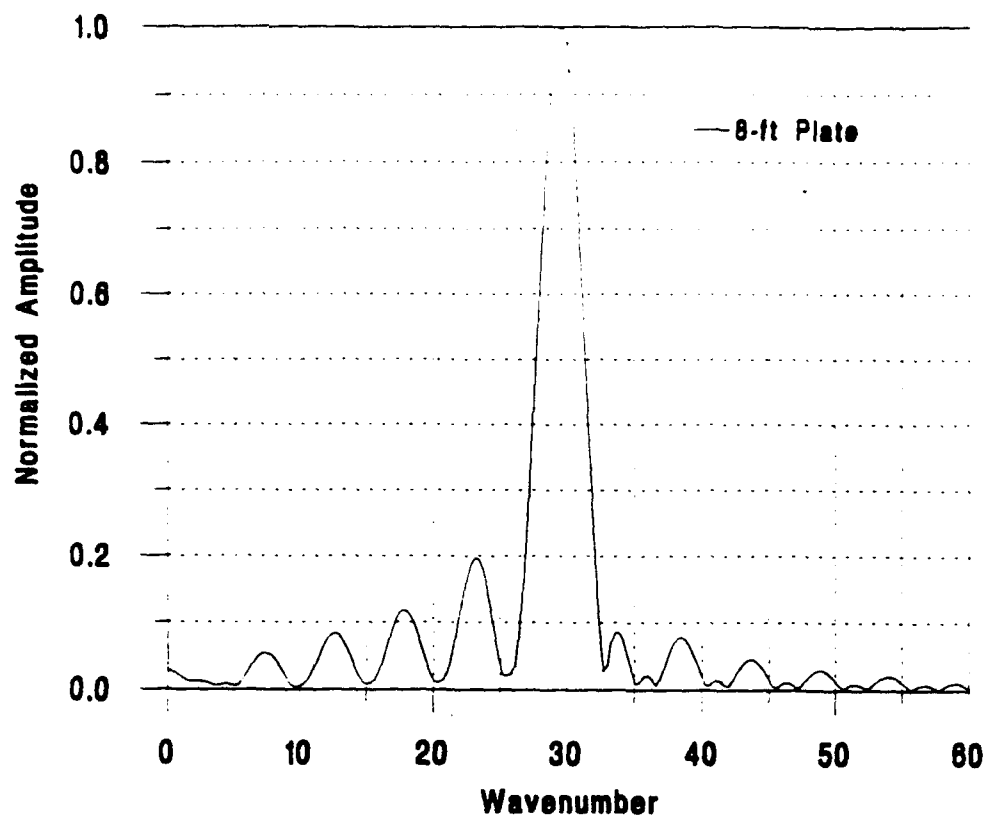
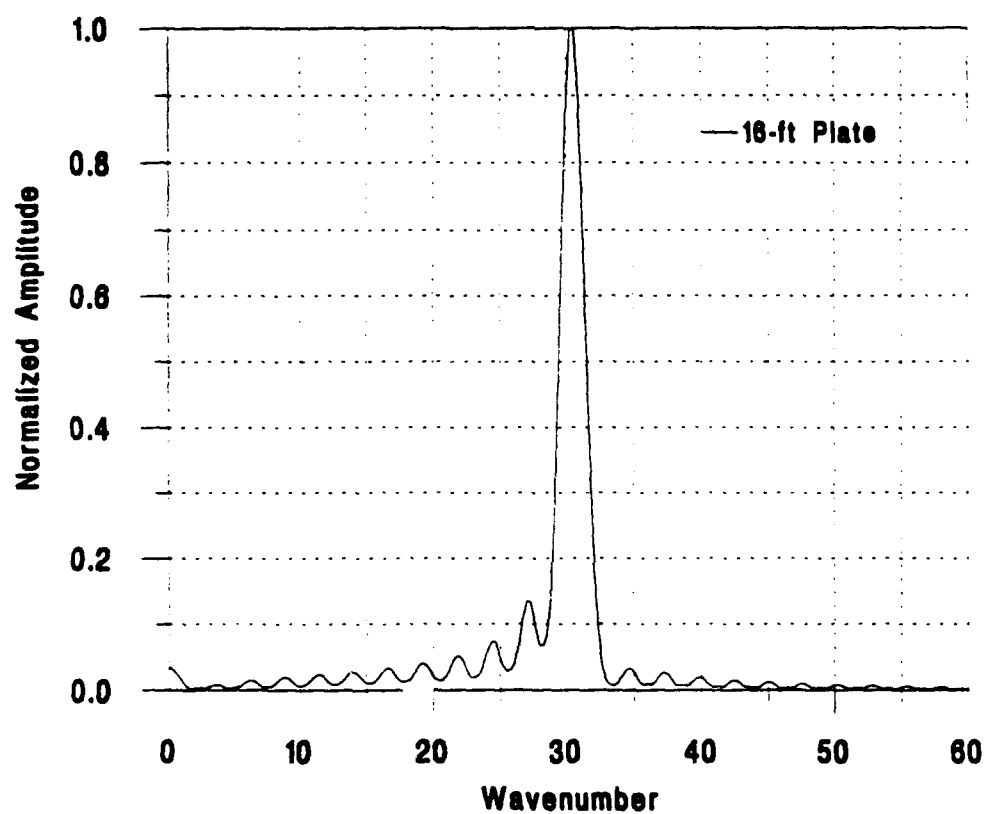Figure 8(a). Normalized k-Spectrum for 8-ft (2.4384m) Plate at 407Hz.

Figure 8(b). Normalized k-Spectrum for 16-ft (4.8768m) Plate at 407H_{z}
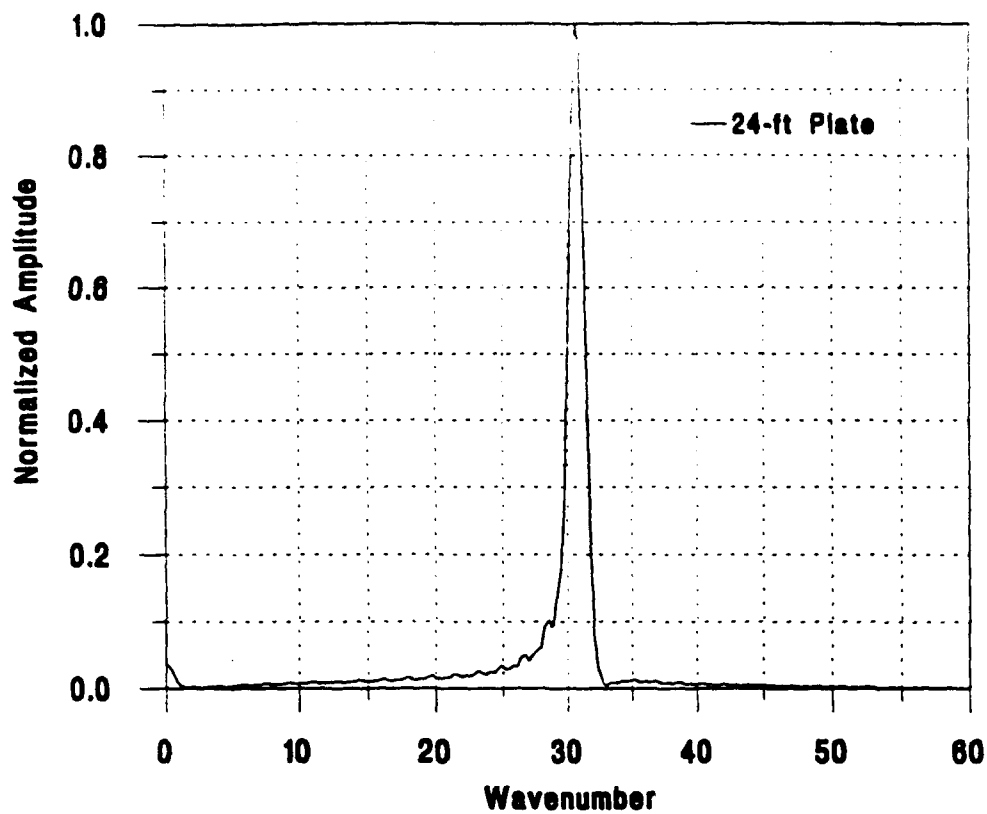
Figure 8(c). Normalized k-Spectrum for 24-*ft* (7.3152*m*) Plate at 407*Hz*.
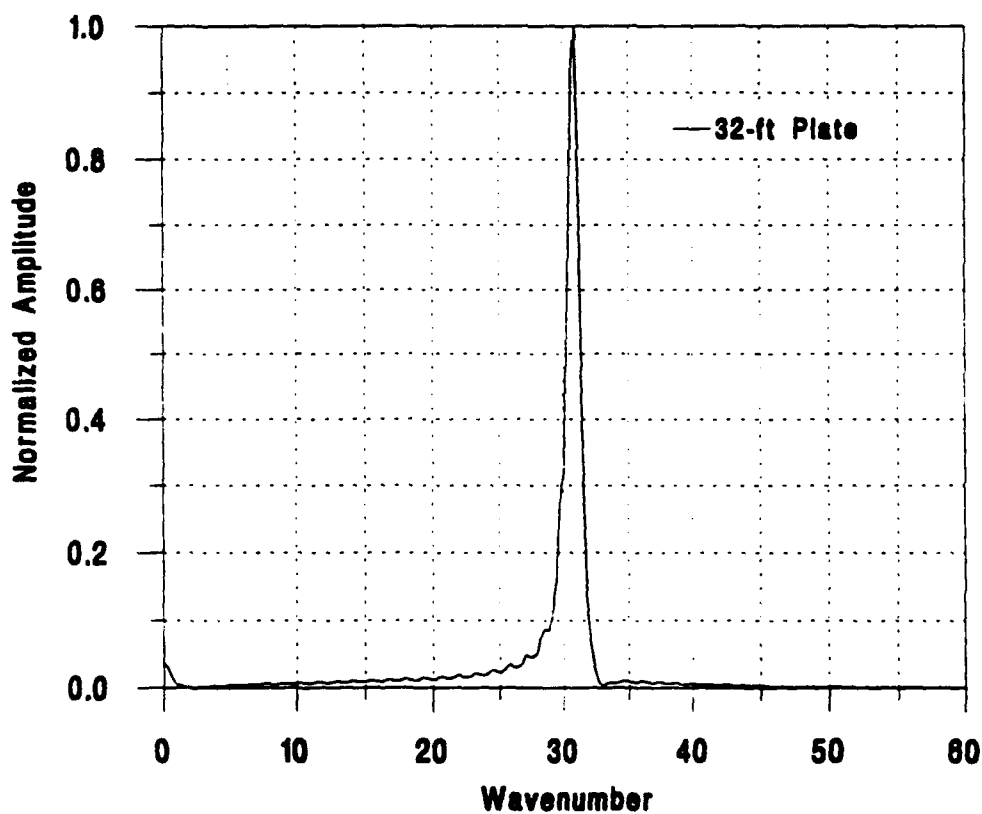

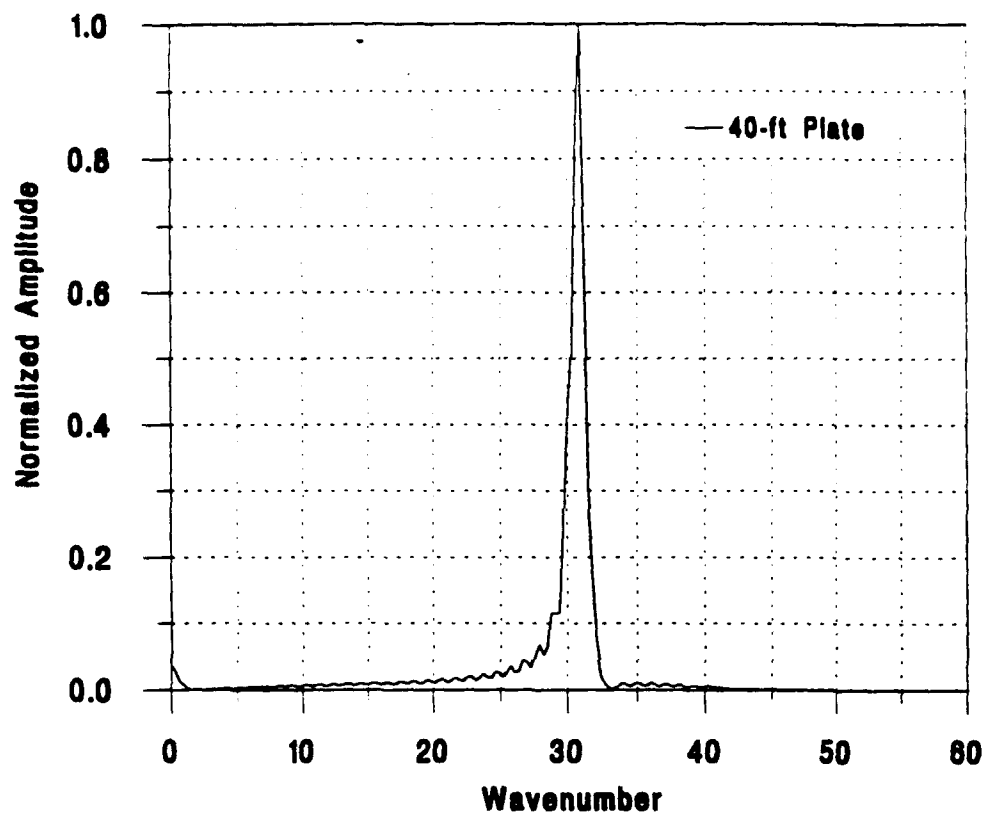Figure 8(d). Normalized k-Spectrum for 32-*ft* (9.7536*m*) Plate at 407*Hz*.

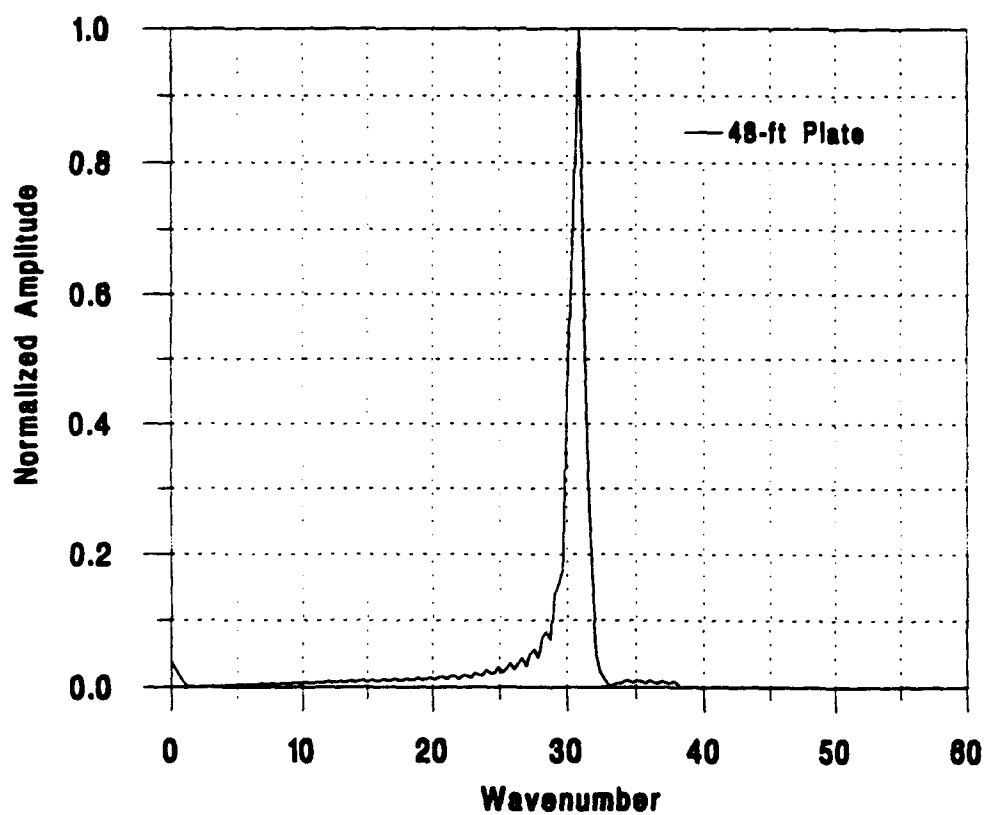Figure 8(e). Normalized *k*-Spectrum for 40-*ft* (12.1920*m*) Plate at 407*Hz*.

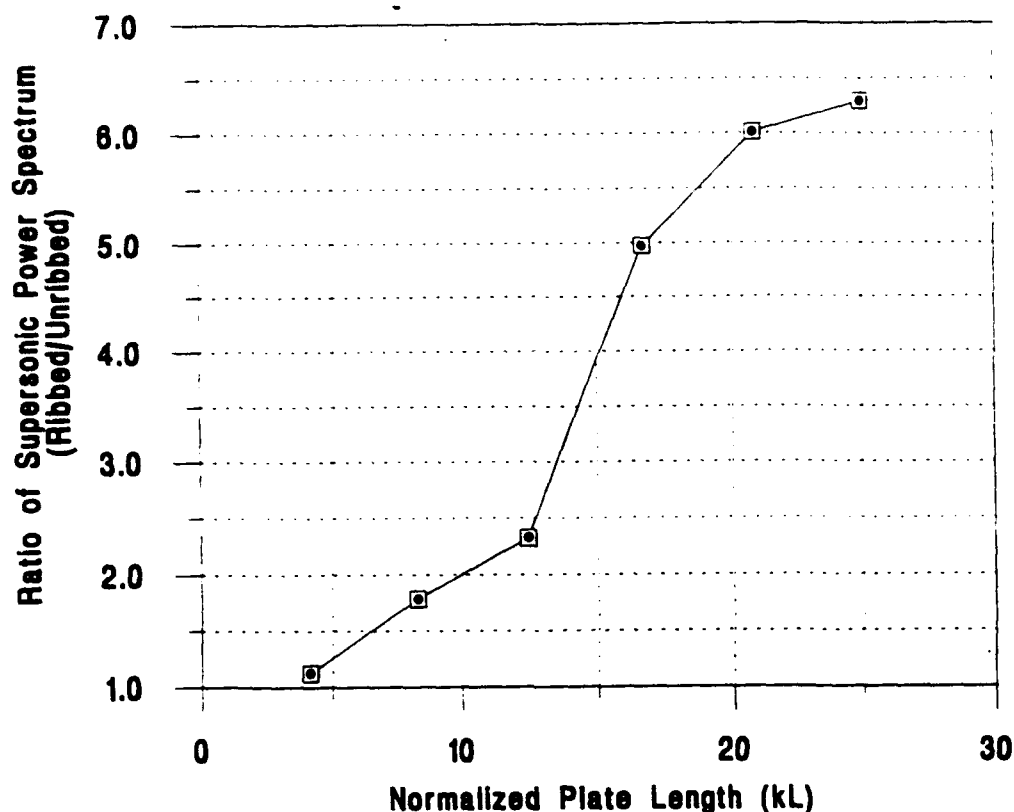Figure 8(f). Normalized *k*-Spectrum for 48-*ft* (14.6304*m*)) Plate at 407*Hz*.

Figure 9. Comparison of Supersonic Power for Ribbed and Unribbed Plates.

IV-3. Directivity Results

One characteristic of a successful acoustic radiator would be its directivity response. In order to demonstrate the effectiveness of attached ribs in enhancing the directive radiation properties of the finite plates examined, far field sound pressure levels were calculated for both the ribbed and unribbed plates. The observation points were located on a line from the mid-length of the plate, coinciding with the force location. The angle was measured from the plane of the plate, so that a value of 90° coincides with the broadside direction. These calculated directivity patterns are shown in Figures 10(a)-10(f). Unlike the unribbed plate, all of the results for the ribbed plate show a pronounced broadside lobe in the radiation pattern. In addition, there are essentially no sidelobes. This radiation pattern is the generally the result of the wavenumber response components at and near $k=0$.
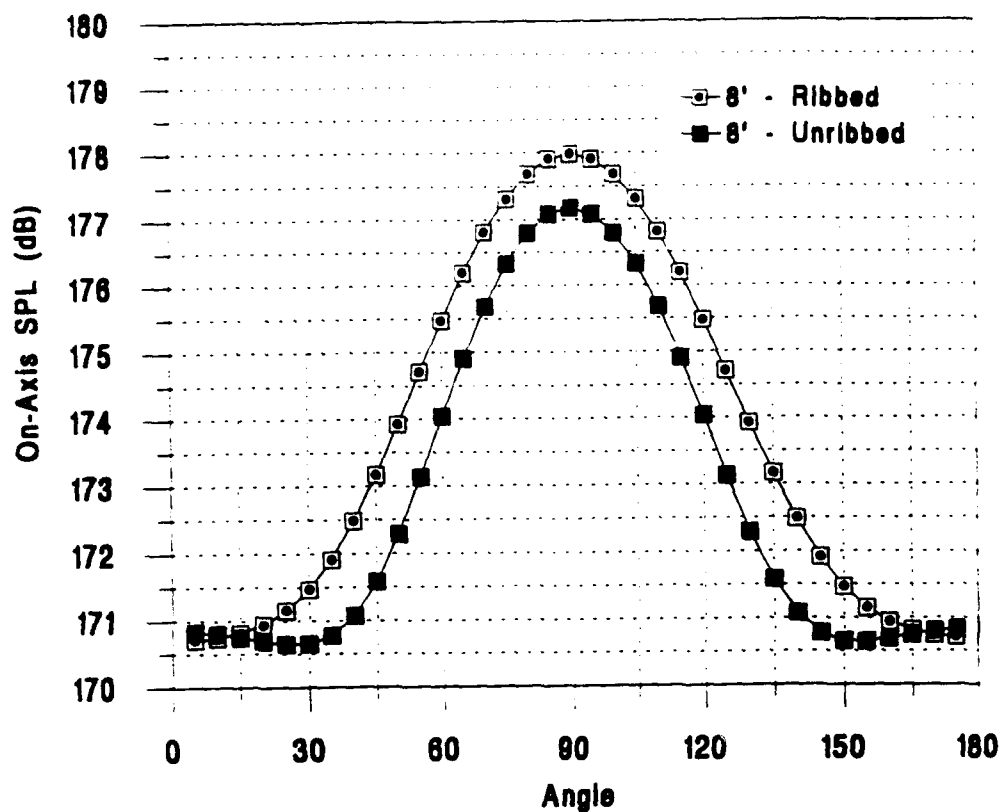
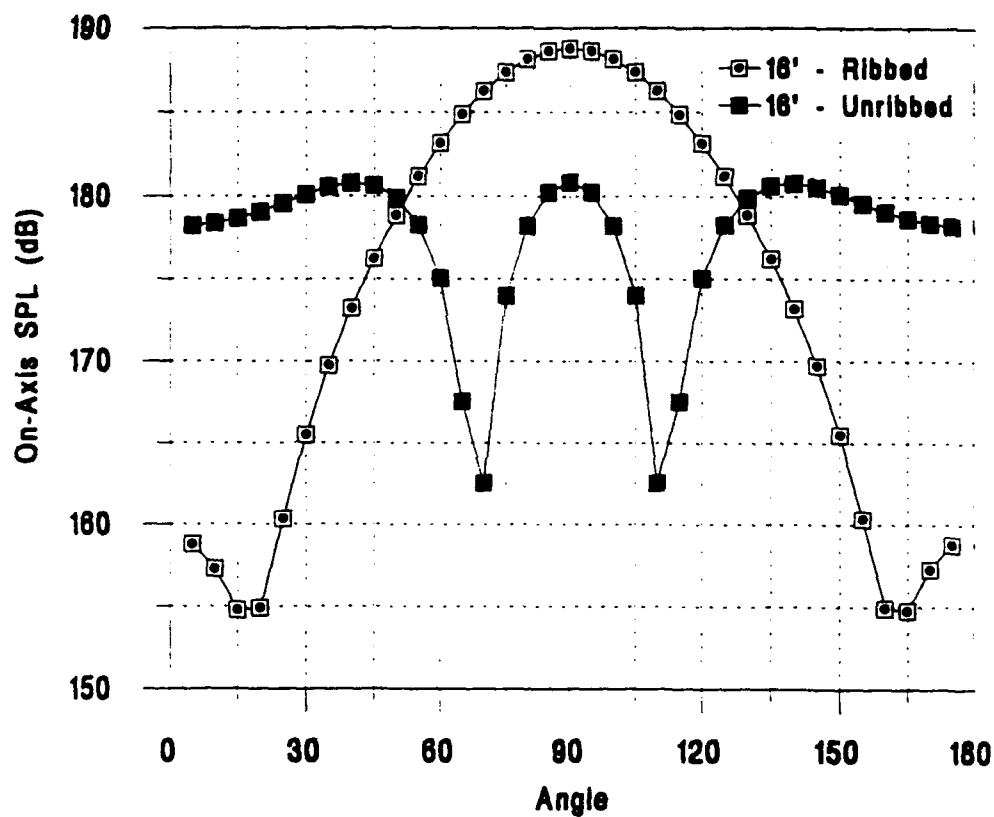Figure 10(a). Directivity Pattern for 8-*ft* (2.4384*m*) Plate at 407*Hz*.

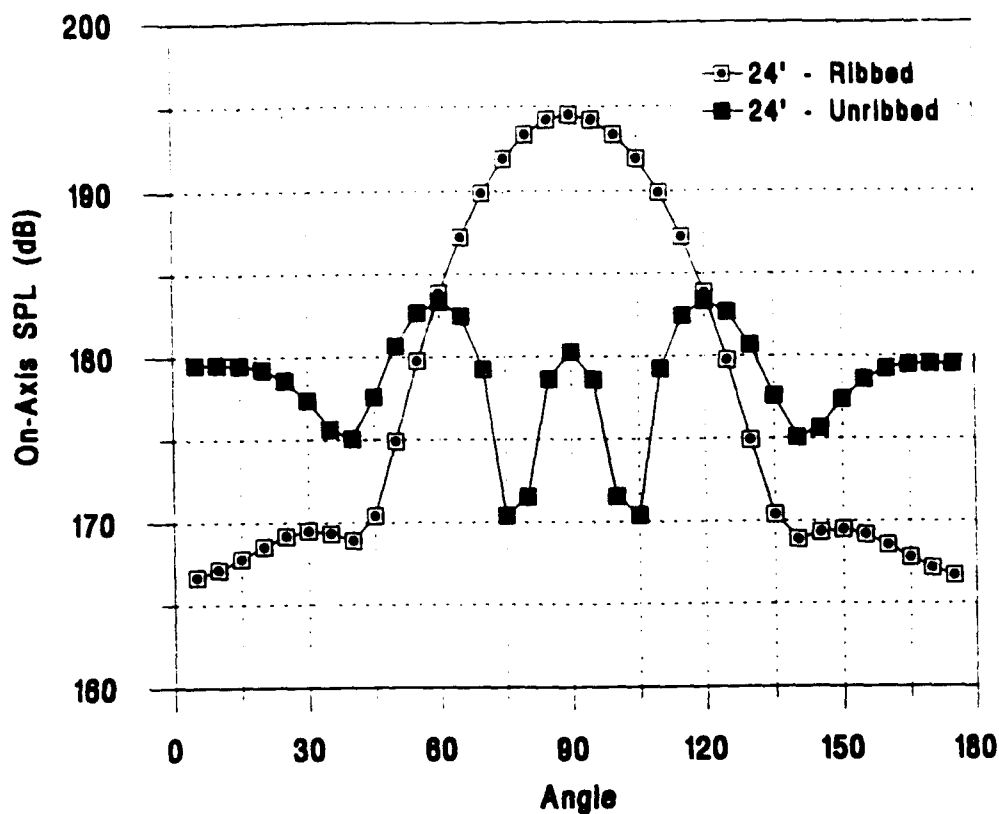Figure 10(b). Directivity Pattern for 16-*ft* (4.8768*m*) Plate at 407*Hz*.

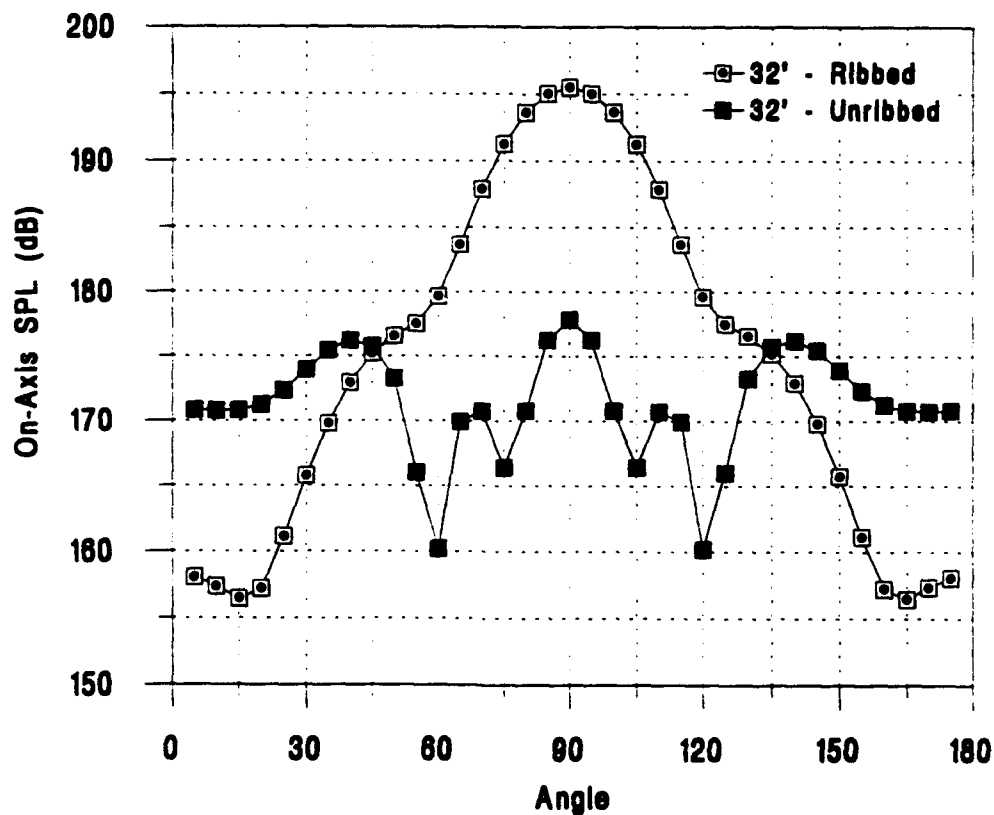Figure 10(c). Directivity Pattern for 24-*ft* (7.3152*m*) Plate at 407*Hz*.

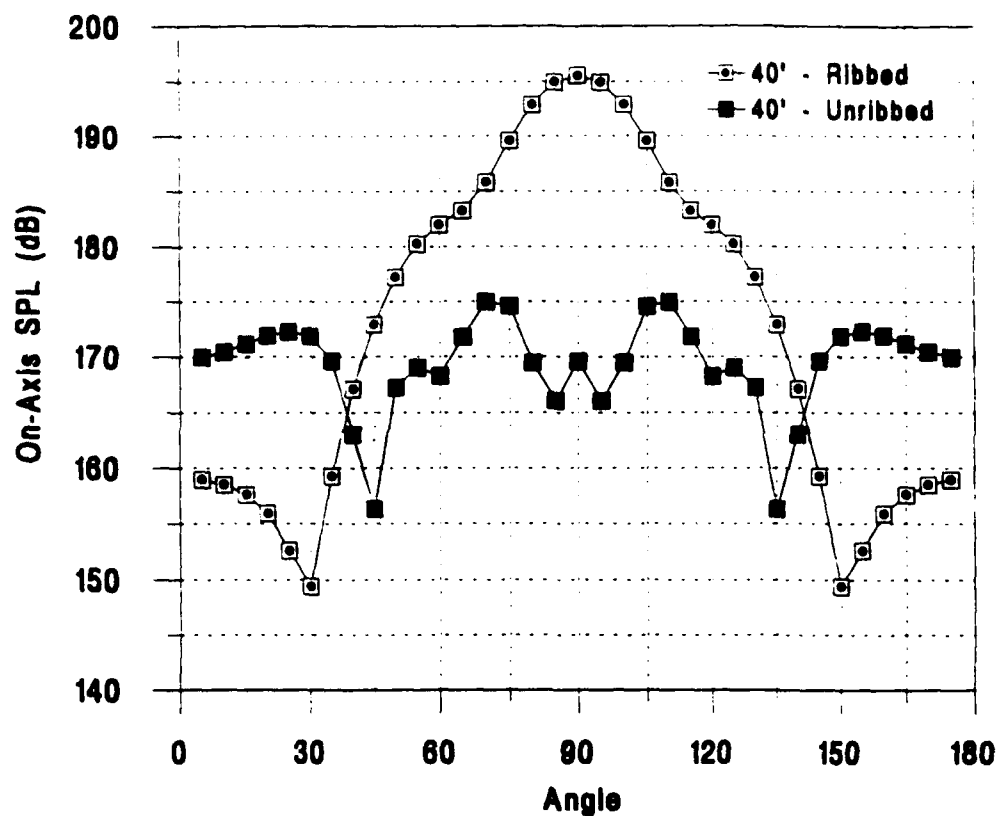Figure 10(d). Directivity Pattern for 32-*ft* (9.7536*m*) Plate at 407*Hz*.

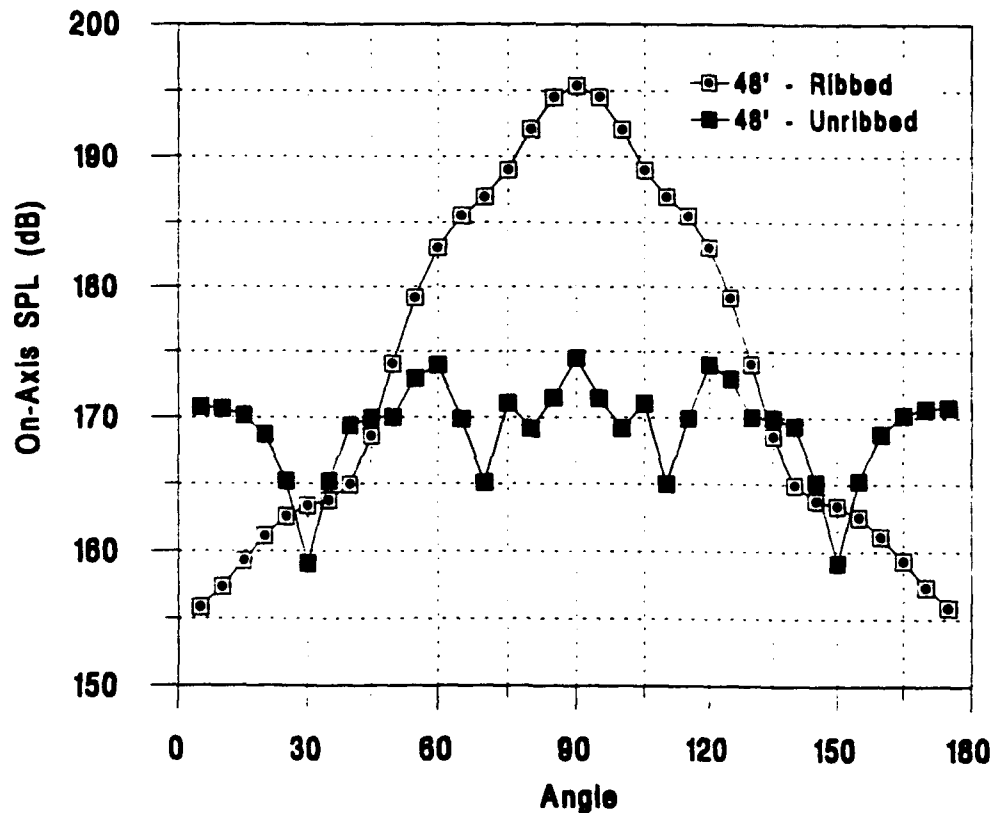Figure 10(e). Directivity Pattern for 40-*ft* (12.1920*m*) Plate at 407*Hz*.

Figure 10(f). Directivity Pattern for 48-*ft* (14.6304*m*)) Plate at 407*Hz*.

It is helpful in quantifying the directivity results to calculate a beam width for each of the ribbed plates. A value of -3*dB* was chosen as a parameterization of the beam width, and the resulting data is shown in Figure 11 as a function of plate length. These results are similar to those noted earlier in that the curve begins to flatten between the 24-*ft* (7.3152*m*, *kL*=12.470) and the 32-*ft* (9.7536*m*, *kL*=16.627) plates.
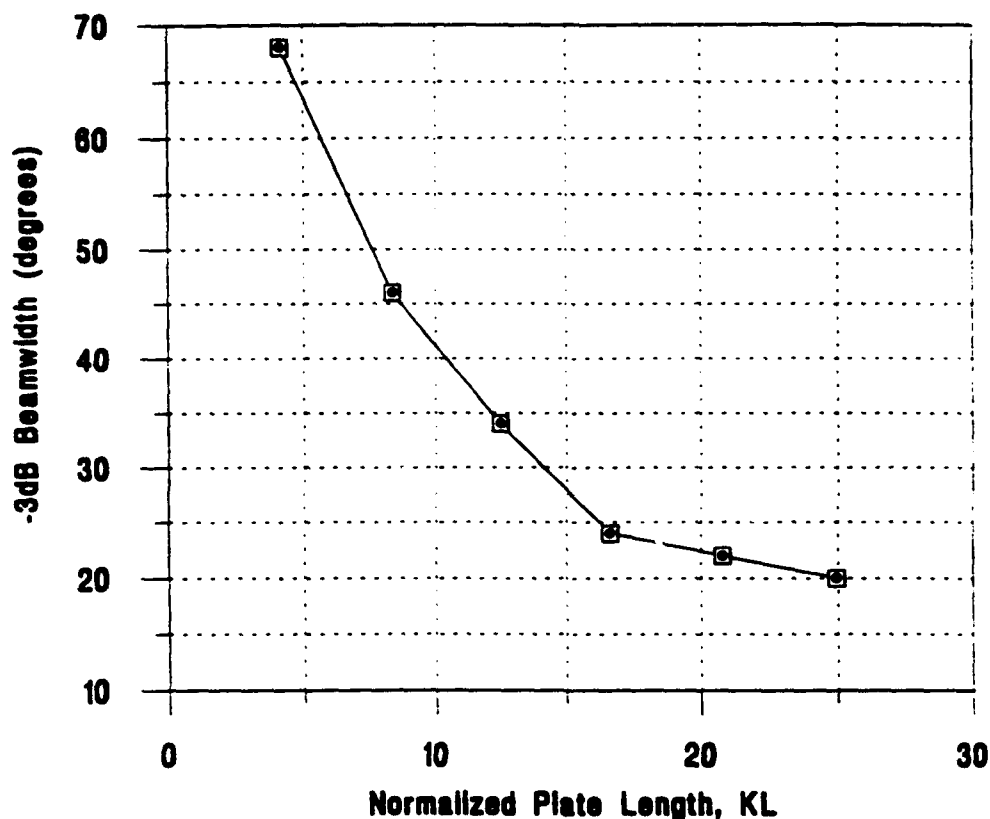

Figure 11. -3dB Beam Width Values for Finite Ribbed Plates at 407*Hz*.

V. Conclusions

This study has shown that the enhanced radiation effects associated with the addition of regularly-spaced stiffeners to an infinite plate are also observed in finite plates. In general, the effects associated with the enhanced radiation, namely increases in both radiated sound pressure level and directivity, track strongly with plate length. It is important, however, to note that there appears to be a 'critical plate length', beyond which

further enhancements are significantly less dramatic. For the candidate geometry considered in this study, it was found that a plate approximately 28-*ft* (8.5344*m*) long demonstrated radiated sound levels and directivity values at 407*Hz* nearly identical with those observed from the infinite plate model. In addition, the results demonstrated that the wavenumber spectrum of the finite plate contained the same critical details as that of the infinite plate.

The overall conclusion from this study is that finite ribbed plates do indeed have potential as enhanced low frequency radiators of sound. This effect is noted at certain frequencies at which the dominant structural response wavenumber coincides with the wavenumber associated with the rib spacing.

VI. References

1. B. Cray, "Near-Field and Far-Field Sound Radiation From a Line-Driven Fluid-Loaded Infinite Flat Plate Having Periodic and Non-Periodic Attached Rib Stiffeners", NUWC-NL Technical Document 10023, March 4, 1992.

2. R.F. Keltie, "The Effects of Rib Stiffeners on the Structural and Acoustic Response of Fluid Loaded Finite Flat Plates", IPA Activity Report to Naval Underwater Systems Center, New London Laboratory, November 1991.

3. R.F. Keltie, "Structural Acoustic Response of Finite Rib-Reinforced Plates", *Journal of the Acoustical Society of America*, 94(1), August, 1993.

4. P.M. Morse and K.U. Ingard, Theoretical Acoustics, 1968, 366.